

Model and simulation of wide-band interaction in free-electron lasers

Yosef Pinhasi *, Yuri Lurie, and Asher Yahalom

The College of Judea and Samaria

Dept. of Electrical and Electronic Engineering

— Faculty of Engineering

P.O. Box 3, Ariel 44837, Israel

16th October 2018

Abstract

A three-dimensional, space-frequency model for simulation of interaction in free-electron lasers (FELs) is presented. The model utilizes an expansion of the total electromagnetic field (radiation and space-charge waves) in terms of transverse eigenmodes of the waveguide, in which the field is excited and propagates. The mutual interaction between the electron beam and the electromagnetic field is fully described by coupled equations, expressing the evolution of mode amplitudes and electron beam dynamics.

Based on the three-dimensional model, a numerical particle simulation code was developed. A set of coupled-mode excitation equations, expressed in the frequency domain, are solved self-consistently with the equations of particles motion. Variational numerical methods were used to simulate excitation of backward modes. At present, the code can simulate free-electron lasers operation in various modes: spontaneous (shot-noise) and self-amplified spontaneous emission (SASE), super-radiance and stimulated emission, all in the non-linear Compton or Raman regimes.

*E-mail adress: yosip@eng.tau.ac.il

1 Introduction

Several numerical models have been suggested for three-dimensional simulation of the FEL operation in the non-linear regime [1]-[10]. Unlike a previously developed steady-state models, in which the interaction is assumed to be at a single frequency (or at discrete frequencies), the approach presented in this paper considers a continuum of frequencies, enabling solution of non-stationary, wide-band interactions in electron devices operating in the linear (small-signal) and non-linear (saturation) regimes. Solution of excitation equations in the space-frequency domain inherently takes into account dispersive effects arising from cavity and beam loading. The model is based on a coupled-mode approach expressed in the frequency domain [11] and used in the WB3D particle simulation code to calculate the total electromagnetic field excited by an electron beam drifting along a waveguide in the presence of a wiggler field of FEL.

The unique features of the present model enable one to solve non-stationary interactions taking place in electron devices such as spontaneous and super-radiant emissions in a pulsed beam FEL, shown in Fig. 1. We employed the code to demonstrate a spontaneous and super-radiant emissions excited when a bunch of electrons passes through a wiggler of an FEL. Calculations of the power and energy spectral distribution in the frequency domain were carried out. The temporal field was found by utilizing a procedure of inverse Fourier transformation. Super-radiance in the special limit of 'grazing' (where dispersive waveguide effects play a role) was also investigated.

2 Dynamics of the particles

The state of the particle i is described by a six-components vector, which consists of the particle's position coordinates $\mathbf{r}_i = (x_i, y_i, z_i)$ and velocity vector \mathbf{v}_i . Here (x, y) are the transverse coordinates and z is the longitudinal axis of propagation. The velocity of each particle, in the presence of electric $\mathbf{E}(\mathbf{r}, t)$ and magnetic $\mathbf{B}(\mathbf{r}, t) = \mu\mathbf{H}(\mathbf{r}, t)$ fields, is found from the Lorentz force equation:

$$\frac{d}{dt} (\gamma_i \mathbf{v}_i) = -\frac{e}{m} [\mathbf{E}(\mathbf{r}_i, t) + \mathbf{v}_i \times \mathbf{B}(\mathbf{r}_i, t)] \quad (1)$$

where e and m are the electron charge and mass respectively. The fields represent the total (DC and AC) forces operating on the particle, and include

also the self-field due to space-charge. The Lorentz relativistic factor γ_i of each particle is found from the equation for kinetic energy:

$$\frac{d\gamma_i}{dt} = -\frac{e}{mc^2} \mathbf{v}_i \cdot \mathbf{E}(\mathbf{r}_i, t) \quad (2)$$

where c is the velocity of light.

The equations are rewritten, such that the coordinate of the propagation axis z becomes the independent variable, by replacing the time derivative $\frac{d}{dt} = v_{zi} \frac{d}{dz}$. This defines a transformation of variables for each particle, which enables one to write the three-dimensional equations of motion in terms of z :

$$\frac{d\mathbf{v}_i}{dz} = \frac{1}{\gamma_i} \left\{ -\frac{e}{m} \frac{1}{v_{zi}} [\mathbf{E}(\mathbf{r}_i, t) + \mathbf{v}_i \times \mathbf{B}(\mathbf{r}_i, t)] - \mathbf{v}_i \frac{d\gamma_i}{dz} \right\} \quad (3)$$

$$\frac{d\gamma_i}{dz} = -\frac{e}{mc^2} \frac{1}{v_{zi}} \mathbf{v}_i \cdot \mathbf{E} \quad (4)$$

The time it takes a particle to arrive at a position z , is a function of the time t_{0i} when the particle entered at $z = 0$, and its instantaneous longitudinal velocity $v_{zi}(z)$ along the path of motion:

$$t_i(z) = t_{0i} + \int_0^z \frac{1}{v_{zi}(z')} dz' \quad (5)$$

3 The driving current

The distribution of the current in the beam is determined by the position and the velocity of the particles:

$$\begin{aligned} \mathbf{J}(\mathbf{r}, t) &= -\sum_i q_i \mathbf{v}_i \delta(x - x_i) \delta(y - y_i) \delta[z - z_i(t)] = \\ &= -\sum_i q_i \left(\frac{\mathbf{v}_i}{v_{zi}} \right) \delta(x - x_i) \delta(y - y_i) \delta[t - t_i(z)] \end{aligned} \quad (6)$$

here q_i is the charge of the i th macro particle in the simulation. The Fourier transform (in the positive frequency domain) of the current density is given by:

$$\begin{aligned} \tilde{\mathbf{J}}(\mathbf{r}, f) &= 2u(f) \int_{-\infty}^{+\infty} \mathbf{J}(\mathbf{r}, t) e^{-j2\pi f t} dt = \\ &= -2u(f) \sum_i q_i \left(\frac{\mathbf{v}_i}{v_{zi}} \right) \delta(x - x_i) \delta(y - y_i) e^{-j2\pi f t_i(z)} \end{aligned} \quad (7)$$

here $u(f) = \begin{cases} 1, & f \geq 0 \\ 0, & f < 0 \end{cases}$ is the step function.

This Fourier transform of the current (7) is substituted in the following excitation equations to find the evolution of the electromagnetic fields.

4 The electromagnetic field

The Fourier transform of the transverse component of the total electromagnetic field is given at the frequency domain as a superposition of waveguide transverse eigenmodes

$$\begin{aligned}\tilde{\mathbf{E}}_{\perp}(\mathbf{r}, f) &= \sum_q \left\{ C_{+q}(z, f) e^{-jk_{zq}z} + C_{-q}(z, f) e^{+jk_{zq}z} \right\} \tilde{\mathcal{E}}_{q\perp}(x, y) \\ \widetilde{\mathbf{H}}_{\perp}(\mathbf{r}, f) &= \sum_q \left\{ C_{+q}(z, f) e^{-jk_{zq}z} - C_{-q}(z, f) e^{+jk_{zq}z} \right\} \widetilde{\mathcal{H}}_{q\perp}(x, y)\end{aligned}\quad (8)$$

and the expression for the longitudinal component of the electromagnetic field is found to be:

$$\begin{aligned}\tilde{E}_z(\mathbf{r}, f) &= \sum_q \left\{ C_{+q}(z, f) e^{-jk_{zq}z} - C_{-q}(z, f) e^{+jk_{zq}z} \right\} \tilde{\mathcal{E}}_{qz}(x, y) + \frac{j}{2\pi f \varepsilon} \tilde{J}_z(\mathbf{r}, f) \\ \widetilde{H}_z(\mathbf{r}, f) &= \sum_q \left\{ C_{+q}(z, f) e^{-jk_{zq}z} + C_{-q}(z, f) e^{+jk_{zq}z} \right\} \widetilde{\mathcal{H}}_{qz}(x, y)\end{aligned}\quad (9)$$

Where $k_{zq} = \sqrt{\left(\frac{2\pi f}{c}\right)^2 - k_{\perp q}^2}$ ($k_{\perp q}$ is the cut-off wave number of mode q) and $C_{+q}(z, f)$ and $C_{-q}(z, f)$ are the q th mode's amplitude corresponding to the forward and backward waves, respectively. Equations (8) and (9) describe the total transverse and longitudinal electromagnetic field (radiation and space-charge waves) [11].

The evolution of the q th mode amplitudes $C_{\pm q}(z, f)$ is found after substitution of the current distribution (7) into the scalar differential excitation equation:

$$\begin{aligned}\frac{d}{dz} C_{\pm q}(z, f) &= \\ &= \mp \frac{1}{2\mathcal{N}_q(f)} e^{\pm jk_{zq}z} \int \int \left[\left(\frac{Z_q}{Z_q^*} \right) \tilde{\mathbf{J}}_{\perp}(\mathbf{r}, f) + \hat{\mathbf{z}} \tilde{J}_z(\mathbf{r}, f) \right] \cdot \tilde{\mathcal{E}}_{\pm q}^*(x, y) dx dy =\end{aligned}$$

$$= \pm \frac{1}{\mathcal{N}_q(f)} e^{\pm j k_{zq} z} \sum_i q_i e^{-j 2\pi f t_i(z)} \left\{ \frac{\zeta_q}{v_{z_i}} \mathbf{v}_{\perp i} \cdot \tilde{\mathcal{E}}_{\pm q \perp}^*(x_i, y_i) + \tilde{\mathcal{E}}_{\pm q z}^*(x_i, y_i) \right\} \quad (10)$$

here

$$\mathcal{N}_q(f) = \int \int [\tilde{\mathcal{E}}_{q \perp} \times \tilde{\mathcal{H}}_{q \perp}^*] \cdot \hat{\mathbf{z}} \, dx \, dy$$

is the power normalization of mode q , and

$$\zeta_q \equiv \frac{Z_q}{Z_q^*} = \begin{cases} +1, & \text{propagating modes} \\ -1, & \text{cut-off modes} \end{cases}$$

The total electromagnetic field is found by inverse Fourier transformation of (8) and (9):

$$\begin{aligned} \mathbf{E}(\mathbf{r}, t) &= \Re \left\{ \int_0^\infty \tilde{\mathbf{E}}(\mathbf{r}, f) e^{+j 2\pi f t} df \right\} \\ \mathbf{H}(\mathbf{r}, t) &= \Re \left\{ \int_0^\infty \tilde{\mathbf{H}}(\mathbf{r}, f) e^{+j 2\pi f t} df \right\} \end{aligned} \quad (11)$$

The energy flux spectral distribution (defined in the positive frequency domain $f \geq 0$) is given by:

$$\begin{aligned} \frac{dW(z)}{df} &= \frac{1}{2} \Re \left\{ \int \int [\tilde{\mathbf{E}}(\mathbf{r}, f) \times \tilde{\mathbf{H}}^*(\mathbf{r}, f)] \cdot \hat{\mathbf{z}} \, dx \, dy \right\} = \\ &= \frac{1}{2} \sum_q^{\text{Propagating}} [|C_{+q}(z, f)|^2 - |C_{-q}(z, f)|^2] \Re \{ \mathcal{N}_q(f) \} \\ &\quad + \sum_q^{\text{Cut-off}} \Im \{ C_{+q}(z, f) C_{-q}^*(z, f) \} \Im \{ \mathcal{N}_q(f) \} \end{aligned} \quad (12)$$

5 The Variational Principle

The solution of the equations (3), (4) and (10) for forward waves is done by integrating the equations in the positive z -direction for a given boundary conditions at the point $z = 0$. For backward waves the natural physical boundary conditions are given at the end of the interaction region $z = L_w$ and the direction of the integration is the negative z -direction.

In order to take into account excitation of both forward and backward waves, we introduce a variational functional

$$\begin{aligned}
F &= \\
&= \int_0^{L_w} \left[C_{-q}(z, f) \frac{dC_{+q}(z, f)}{dz} - C_{+q}(z, f) \alpha_q(z, f) + C_{-q}(z, f) \beta_q(z, f) \right] dz
\end{aligned} \tag{13}$$

where

$$\begin{aligned}
\alpha_q(z, f) &= \\
&= -\frac{1}{2\mathcal{N}_q(f)} e^{-jk_{zq}z} \iint \left[\left(\frac{Z_q}{Z_q^*} \right) \tilde{\mathbf{J}}_{\perp}(\mathbf{r}, f) + \hat{\mathbf{z}} \tilde{J}_z(\mathbf{r}, f) \right] \cdot \tilde{\mathcal{E}}_{-q}^*(x, y) dx dy \\
\beta_q(z, f) &= \\
&= +\frac{1}{2\mathcal{N}_q(f)} e^{+jk_{zq}z} \iint \left[\left(\frac{Z_q}{Z_q^*} \right) \tilde{\mathbf{J}}_{\perp}(\mathbf{r}, f) + \hat{\mathbf{z}} \tilde{J}_z(\mathbf{r}, f) \right] \cdot \tilde{\mathcal{E}}_{+q}^*(x, y) dx dy
\end{aligned} \tag{14}$$

The variational derivative of the above functional is:

$$\begin{aligned}
\delta F &= \int_0^{L_w} \left[\delta C_{-q}(z, f) \left(\frac{dC_{+q}(z, f)}{dz} + \beta_q(z, f) \right) \right. \\
&\quad \left. - \delta C_{+q}(z, f) \left(\frac{dC_{-q}(z, f)}{dz} + \alpha_q(z, f) \right) + \frac{d(C_{-q}(z, f) \delta C_{+q}(z, f))}{dz} \right] dz
\end{aligned} \tag{15}$$

For arbitrary variations $\delta C_{\pm q}(z, f)$ the functional minimizes (i.e., $\delta F = 0$) if and only if the equations (10) are satisfied, and the boundary term is

$$\delta F_B = \int_0^{L_w} \frac{d(C_{-q}(z, f) \delta C_{+q}(z, f))}{dz} dz = C_{-q}(z, f) \delta C_{+q}(z, f) \Big|_0^{L_w} = 0 \tag{16}$$

resulting in

$$C_{-q}(0, f) \delta C_{+q}(0, f) = C_{-q}(L_w, f) \delta C_{+q}(L_w, f) \tag{17}$$

This enable solving amplifier scheme in which the boundary conditions are $C_{-q}(L_w, f) = 0$ and $C_{+q}(0, f) = 0$, as well as an oscillator configuration where the boundary conditions are $C_{-q}(0, f) = C_{-q}(L_w, f)$ and $C_{+q}(0, f) = C_{+q}(L_w, f)$.

6 Numerical results

We shall use the code to investigate super-radiant emission radiated when an ultra short e -beam bunch (with duration of 1 pS, much shorter than the temporal period of the signal) passes through the wiggler of an FEL having operational parameters as given in table 1. In this case, the power of super-radiant (coherent) emission is much higher than that of the incoherent spontaneous emission [12].

Fig. 2 shows two cases of dispersion relations: when the beam energy is set to 1.375 MeV, there are two separated intersection points between the beam and waveguide dispersion curves, corresponding to the “slow” ($v_{g1} < v_{z0}$) and “fast” ($v_{g2} > v_{z0}$) synchronism frequencies 29 GHz and 100 GHz, respectively. Lowering the beam energy to 1.066 MeV, results in a single intersection (at 44 GHz), where the beam dispersion line is tangential to the waveguide dispersion curve ($v_g = v_{z0}$ — “grazing limit”).

The calculated spectral density of energy flux in the case of two well-separated solutions is shown in Fig. 3a. The spectrum peaks at the two synchronism frequencies with main lobe bandwidth of $\Delta f_{1,2} \approx \frac{1}{\tau_{sp1,2}}$, where $\tau_{sp1,2} \approx \left| \frac{L_w}{v_{z0}} - \frac{L_w}{v_{g1,2}} \right|$ is the slippage time. The corresponding temporal wavepacket (shown in Fig. 3b) consist of two “slow” and “fast” pulses with durations equal to the slippage times modulating carriers at their respective synchronism frequencies. The spectral bandwidth in the case of grazing shown in Fig. 4a, is determined by dispersive effects of the waveguide taking into account by the simulation. The corresponding temporal wavepacket is shown in Fig. 4b.

Acknowledgments

The research of the second author (Yu. L.) was supported in part by the Center of Scientific Absorption of the Ministry of Absorption, State of Israel.

References

- [1] W. M. Fawley, D. Prosnitz and E. T. Scharlemann, *Phys. Rev. A* **30**, 2472 (1984)
- [2] B. D. McVey, *Nucl. Instrum. Methods Phys. Res. A* **250**, 449 (1986)

- [3] A. K. Ganguly and H. P. Freund, *Phys. fluids* **31**, 387 (1988)
- [4] S. Y. Cai, A. Bhattacharjee and T. C. Marshall, *Nucl. Instrum. Methods Phys. Res. A* **272**, 481 (1988)
- [5] T. M. Tran and J. S. Wurtele, *Computer Physics Comm.* **54**, 263 (1989)
- [6] T.-M. Tran and J. S. Wurtele, *Phys. Reports* **195** (1990)
- [7] M. Caplan, *Nucl. Instrum. Methods Phys. Res. A* **318**, 655 (1992)
- [8] M. Caplan et al., *Nucl. Instrum. Methods Phys. Res. A* **331**, 243 (1993)
- [9] Pallavi Jha and J. S. Wurtele, *Nucl. Instrum. Methods Phys. Res. A* **331**, 243 (1993)
- [10] Y. Pinhasi, A. Gover, and V. Shterngartz, *Phys. Rev. E* **54**, 6774 (1996)
- [11] Y. Pinhasi and A. Gover, *Phys. Rev. E* **48**, 3925 (1993)
- [12] Y. Pinhasi, Yu. Lurie: “Generalized theory and simulation of spontaneous and super-radiant emissions in electron devices and free-electron lasers”, accepted for publication in *Phys. Rev. E*.

Table 1: The operational parameters of millimeter wave free-electron maser.

Accelerator

Electron beam energy:	$E_k=1\div 3$ MeV
Electron beam current:	$I_0=1$ A
Pulse duration:	$T=1$ pS

Wiggler

Magnetic induction:	$B_w=2000$ G
Period:	$\lambda_w=4.444$ cm
Number of periods:	$N_w=20$

Waveguide

Rectangular waveguide:	1.01 cm \times 0.9005 cm
Mode:	TE_{01}

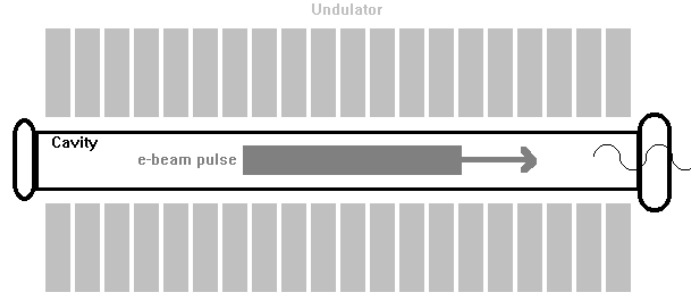


Figure 1: The FEL scheme

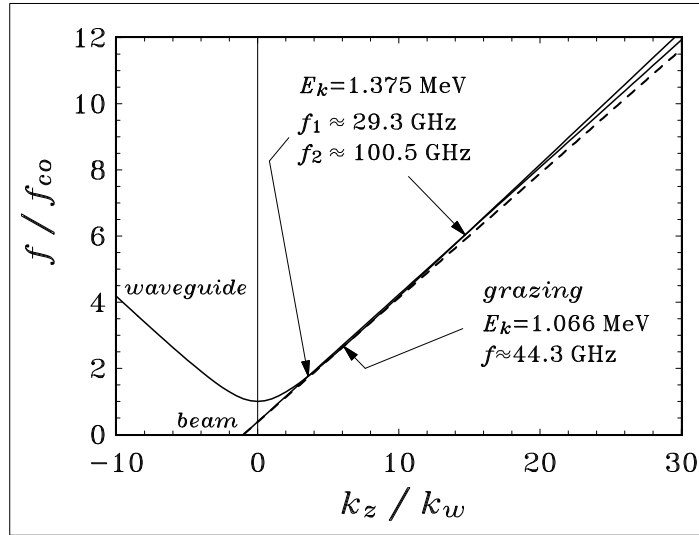


Figure 2: FEL dispersion curves

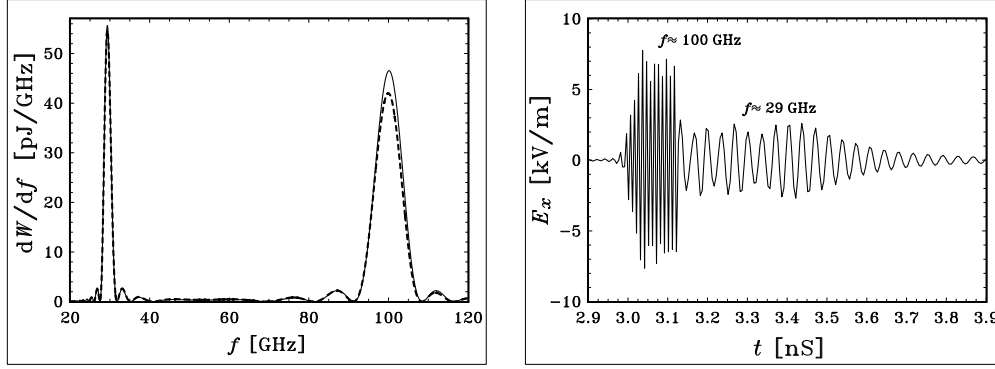


Figure 3: Super-radiant emission from an ultra short bunch: (a) Energy spectrum (analytic calculation and numerical simulation are shown by solid and dashed lines, respectively); (b) temporal wavepacket.

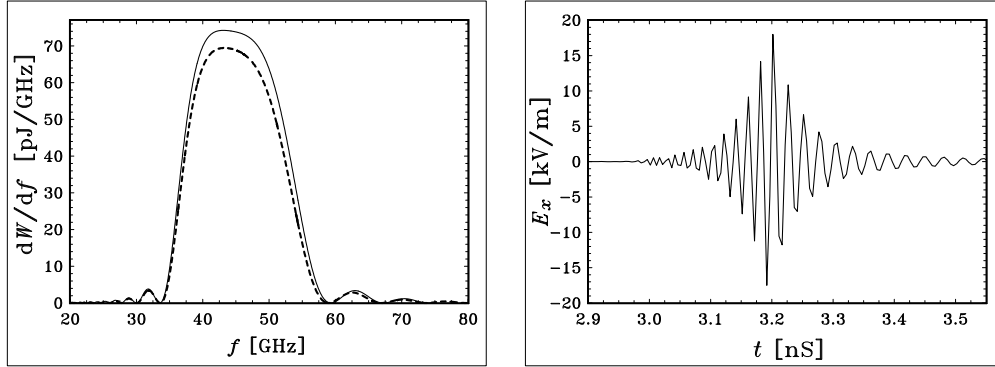


Figure 4: That of Fig. 3, but in the grazing limit.

